Multifocus Image Fusion Algorithm Using Iterative Segmentation based on Edge Information and Adaptive Threshold

Parul Shah, Amy Kumar, Shabbir N. Merchant
Department of Electrical Engineering
IIT Bombay, India
Email: parul,merchant@ee.iitb.ac.in, amy.kumar12@gmail.com

Uday B. Desai
Director
IIT Hyderabad,India
Email: ubdesai@iith.ac.in

***Abstract*—This paper presents algorithm for multifocus image fusion in spatial domain based on iterative segmentation and edge information of the source images. The basic idea is to divide the images into smaller blocks, gather edge information for each block and then select the region with greater edge information to construct the resultant *'all-in-focus'* fused image. To improve the fusion quality further, an iterative approach is proposed. Each iteration selects the regions in focus with the help of an adaptive threshold while leaving the remaining regions for analysis in the next iteration. A further enhancement in the technique is achieved by making the number of blocks and size of blocks adaptive in each iteration. The pixels which remain unselected till the last iteration are then selected from the source images by comparison of the edge activities in the corresponding segments of the source images. The performance of the method have been extensively tested on several pairs of multifocus images and compared quantitatively with existing methods. Experimental results show that the proposed method improves fusion quality by reducing loss of information by almost 50% and noise by more than 99%.**
***Keywords:* Image fusion, Multifocus images, Edge Information.**

I. Introduction

The concept of Image Fusion has been widely used in a wide variety of applications like medicine, satellite imaging, remote sensing, machine vision, automatic change detection, biometrics etc. Image fusion is a concept of combining multiple images into one single image containing more information than that of individual source images. With the existing image-capturing devices, it is not always possible to obtain a single image with all the desired information. When capturing an image of a three dimensional scene it is desirable to have all the objects in the scene to be in focus.

However, it is not always feasible to capture an *all-in-focus* image; since optical lenses of imaging sensor, especially with long focal length, only have a limited depth of field. The goal of image fusion is to integrate complementary multi sensor, multi temporal and/or multi view data into a new image containing all the necessary information from the various source images. In case of multifocus image fusion, the aim is to obtain an all-in-focus image by acquiring information from different focal planes of the various source images and fusing them together into one single image where all the objects in the scene appear to be in focus.

In this paper a novel approach to multifocus image fusion have been proposed based on region based edge information of the source images. At first, the source images are segmented into smaller blocks. Then edge information of each block is gathered and selection of any block from the source images is done by comparison of the corresponding edge activity. Next, we introduces an adaptive threshold for comparison between the corresponding regions of the source images. Lastly, an iterative method is proposed to facilitate the division of required regions into appropriate number of blocks and subsequent selection of block based on an efficient adaptive threshold for comparison. Each iteration preserves the sub-blocks of the source images which are in focus and then passes the remaining regions to the next iteration. The resultant fused images are both quantitatively and visually better than those produced by various other algorithms. Section II gives overview of some of the classical as well as recent image fusion techniques. Section III and IV describes the proposed fusion approaches. Quantitative parameters used for the performance evaluations are reported in Section V. The experimental results (quantitative and visual) are provided and analyzed in the section VI. Section VII concludes the whole paper.

II. Related Work

Image fusion can be as simple as taking pixel-by-pixel average of the source images, but that often leads to undesirable side effects such as reduced contrast. Fusion can broadly be classified as, fusion in frequency domain and in spatial domain. It can be implemented using various fusion rules e.g. $'mean'$ or $'max'$ where fused coefficient is average or maximum of source coefficients respectively. One can also take $'weighted\ average'$ instead, where fused coefficient is weighted average of source coefficients as proposed by [1], [2].

In recent years, various multiscale transforms have become very popular, such as wavelet, wavelet packet, curvelet and contourlet [1], [2], [4]- [8]. In [5], authors have taken weighted average in wavelet domain using fixed weights (0.6 for CT and 0.4 for PET). S. Arivazhagan et. al [2] proposed a wavelet based fusion method for multifocus images using weighted average fusion rule in which, weights are based on local statistical features like mean and standard deviation. Similarly, [6] and [8] have used weights based on local mean and energy to fuse medical and surveillance images respectively in wavelet-packet domain. Soad Ibrahim et. al [7] have fused surveillance images using contourlet and [1] have fused multifocus images combining curvelet and wavelet. Both of them have used $'maximum'$ fusion rule. The basic idea in all these transform based method is to perform a multiresolution decomposition on each source image, then integrate all these decompositions to form a composite representation, and finally reconstruct the fused image by performing an inverse multiresolution transform. This type of algorithm can avoid the discontinuity in the transition zone, but it is computationally expensive. Besides, the frequency algorithm may produce artifacts such as Gibbs phenomenon.

The basic idea of algorithms proposed in this paper is to select an image block from one of the source images, having greater edge information compared to other source image iteratively. The work is mainly focused on finding optimal block size. As the fusion method is in spatial domain we save on time compared to frequency domain techniques which need to transform image to and from frequency domain. Besides, instead of taking weighted average of source pixel, we propose to select one of the source pixel as it is; to avoid blurring caused by 'average' or 'weighted average' fusion rule.

III. Proposed Iterative Fusion with Fixed Block Size and Adaptive Threshold using Edge Information ($FBS - AT$)

Edges characterize boundaries and therefore have a fundamental importance in image processing. Edges in images are areas with strong intensity contrasts a jump in intensity from one pixel to the next. Edge detection of an image significantly reduces the amount of data and filters out useless information, while preserving the important structural properties in an image. In case of multifocus image fusion, if the edge information of the source images is correctly extracted, the subsequent task of interpreting the information content and detecting the in-focus regions becomes a lot easier. There are many ways to perform edge detection. In case of multifocus image fusion, the purpose of extracting edge information is to provide strong visual clues that can help the recognition process and can make a clear distinction between the in-focus regions of the source images. In this paper we have used the canny edge detector [9]. Basic idea is to detect at the zero-crossings of the second directional derivative of the smoothed image in the direction of the gradient where the gradient magnitude of the smoothed image being greater than some threshold depending on image statistics.

Figure 1 shows two source images with complementary regions in focus. Figure 2 shows the edge map of the images in figure 1, using canny edge detection. The threshold has been chosen such that the edge information of only the objects in the in-focus region of the images gets extracted. Hence in

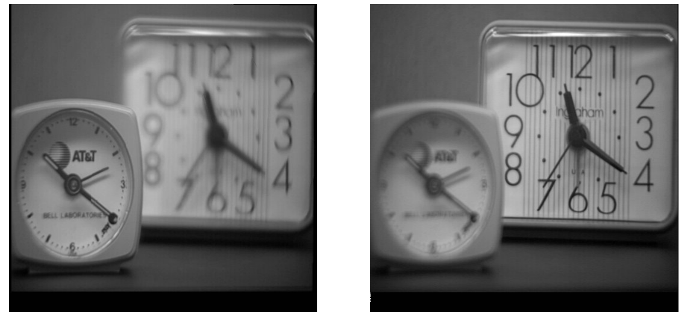

(a) Foreground in focus (b) Background in focus

Fig. 1. Registered multifocus source images of *'clock'* [10]: (a) foreground in focus (b) background in focus

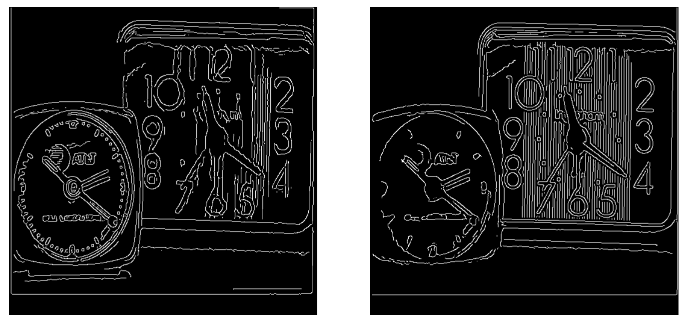

(a) Foreground in focus (b) Background in focus

Fig. 2. Corresponding edge maps of multifocus *'clock'* images using Canny edge detector: (a) foreground in focus (b) background in focus

Figure 2(a), the edges are more prominent in the left region, while in Figure 2(b), the edge information is concentrated to the right.

After extracting the edge information as illustrated in the earlier section, the source images are divided into a fixed number of blocks. The images shown here were divided into 16 blocks. Next, the edge information obtained from the two source images are compared and the image block with higher edge activities are selected to be part of the fused image.

However, that the certain blocks extracted from different source images might contain almost similar number of edges and thus the selection procedure needed to be refined. In this algorithm ($FBS - AT$), selection is made in three iterations described as follows:

1) Firstly, the source images are divided into a certain number of blocks. Then, the difference between edge information from the two source images is computed for each block. Next, the mean of all these differences is calculated and set as the adaptive threshold (T). Now, the differences are compared with this threshold T and only those blocks for which the difference exceeds the threshold are chosen and incorporated into the final fused image from their corresponding source image. The rest of the blocks are passed on to the next iteration. The resultant image at the end of the first iteration for the

(a) (b) (c)

Fig. 3. Resultant image obtained after every iteration of the proposed iterative fusion with fixed block size and adaptive threshold using edge information ($FBS - AT$): (a) first iteration (b) second iteration (c) final fused image

'clock' image pair is shown in Figure 3(a).

2) In the second iteration, the mean of the differences of the regions passed over from the last iteration is calculated and set as the new threshold. Once again, the difference between the number of edge pixels for corresponding image block from different source images, is compared with the threshold, and if the difference is higher than the threshold then the respective block with higher edge information is incorporated into the fused image. The resultant image at the end of the second iteration for the *'clock'* image pair is shown in Figure 3(b).
3) In the third iteration, all the blocks for which no decision has been made are analyzed and the blocks with relatively higher edge information is selected to be part of the fused image. The resultant final fused image for the *'clock'* image pair is shown in Figure 3(c).

IV. Proposed Iterative Algorithm with Adaptive Block Size and Adaptive Threshold ($ABS - AT$)

Fig. 4. Final fused image obtained from the proposed iterative algorithm with adaptive block size and adaptive threshold ($ABS - AT$)

This algorithm is a further enhancement of the proposed $FBS - AT$ algorithm. The improvement here is based on the fact that different images might give different results depending upon the number of blocks they are being divided into. Also, as the analysis proceeds to higher levels of iteration, smaller blocks give better results. Hence in this algorithm, as the iterations change so do the number of divisions. However, the number of divisions are upper-bounded to 256. This in turn decides the lower bound on the size of the blocks. The proposed adaptive threshold concept is used here too. This algorithm can be detailed as follows:

1) The first iteration is carried out in the same way as described in $FBS - AT$ (section III).
2) In the next iteration, the image is divided such that each block is subdivided by twice the number of divisions used in last iteration, i.e. each block of last iteration will be considered as 4 separate blocks. For example, if 10 blocks were passed from the last iteration to the current iteration, these will now be processed in form of 10×4 = 40 blocks. The mean of the differences of edge information from the two source images of these blocks is calculated and set as the new threshold. The regions for which the adaptive threshold criteria is met are incorporated into the final fused image and remaining blocks are passed over to the next iteration. The upper bound on maximum number of divisions and/or minimum block size is set as a control parameter to conclude these iterations and move on to the next stage.
3) At the end of all the iterations of step 2, the blocks for which no decision has been made are analyzed simply by comparing number of respective edge pixels, i.e, for each of these left-over regions, information is taken from the source image which contains higher edge information in that area.

Hence we can say that in this algorithm, the second iteration is expanded to incorporate several other sub- iterations, each with increasing number of divisions performed on the regions passed over from the previous iteration. Also, each of these iterations in step 2, uses a new threshold value calculated using the regions of that iteration, thus making number of blocks and threshold value, both adaptive. The resultant final fused image for the *'clock'* image pair is shown in Figure 4.

V. Quantitative Evaluation Indices of Image Fusion

A fusion artifact introduced into the fused image by the fusion process could lead to a benign object being classified as a threat or a valid target; so an efficient fusion method is one that introduces minimum artifacts. Objective evaluation of fusion quality in the absence of ground truth still does not have a universally accepted solution, and hence is a challenge. Researchers have used and proposed various parameters [1]- [8], [11]- [15], $Petrovic\ Metrics$ being among the most recent ones [15]. To make the exhaustive study, we have considered several classical evaluation parameters so far reported in literature, which are as follows:

1) $Average\ Pixel\ Intensity$ (μ) or mean ($\overline{F}$): an index of contrast.
2) $Average\ Gradient$ ($\overline{G}$): a measure of sharpness and clarity degree.
3) $Standard\ Deviation$ (SD or σ): this is the square root of the variance, which reflects the spread in the data.
4) $Entropy$ (H): an index to evaluate the information quantity in an image.
5) $Mutual\ Information$ (MI) or $Fusion\ Factor$: a measure of correlative information content in fused image with respect to source images.
6) $Fusion\ Symmetry$ (FS) or $Information\ Symmetry$: an indication of how much symmetric the fused image is with respect to source images.
7) Normalized $Correlation$ ($CORR$): a measure of relevance of fused image to source images.
8) $Petrovic\ Metric\ Parameter\ Q_{ABF}$: an index of edge information preservation.
9) $Petrovic\ Metric\ Parameter\ L_{ABF}$: a measure of loss of edge information.
10) $Petrovic\ Metric\ Parameter\ N_{ABF}$: a measure of noise or artifacts added due to

The first seven parameters are computed using equations 1 to 8, assuming ($m \times n$) image size. All the $Petrovic\ Metrics$ are computed as described in [15].

$$\mu = \overline{F} = \frac{\sum_{i=1}^{m}\sum_{j=1}^{n} f(i,j)}{m \times n} \tag{1}$$

Here $f(i,j)$ is pixel intensity for position (i,j) of image F.

$$\overline{G} = \frac{\sqrt{\sum_i \sum_j (f(i,j) - f(i+1,j))^2 + (f(i,j) - f(i,j+1))^2}}{m \times n} \tag{2}$$

$$Entropy = -\sum_{f=0}^{255} p_F(f) log_2 p_F(f) \tag{3}$$

where $p_F(f)$ stands for probability of intensity value f in image F.

$$MI_{AF} = \sum_a \sum_f p_{A,F}(a,f) log_2 \frac{p_{A,F}(a,f)}{p_A(a) p_F(f)} \tag{4}$$

$$MI_{AB}^F = MI_{AF} + MI_{BF} \tag{5}$$

MI_{AF} and MI_{BF} quantify mutual information between source image A and fused image F and, source image B and fused image F respectively. MI_{AB}^F is a measure of overall mutual information between source images and fused image.

$$FS = 2 - |MI_{AF}/(MI_{AF} + MI_{BF}) - 0.5| \tag{6}$$

If the fused image is equally symmetric to both the source images, value of FS will be closer to 2 and the fusion quality will be better.

$$r_{AF} = \frac{\sum_i \sum_j (a(i,j) - \overline{A})(f(i,j) - \overline{F})}{\sqrt{((\sum_i \sum_j (a(i,j) - \overline{A})^2) \sum_i \sum_j (f(i,j) - \overline{F})^2)}} \tag{7}$$

Here r_{AF} and r_{BF} represents normalized correlation between source images and fused image, and $CORR$ stands for overall average normalized correlation.

$$CORR = (r_{AF} + r_{BF})/2 \tag{8}$$

Theoretically, for parameters 1 to 8: higher the value, better is the quality of fused image; whereas for remaining parameters (L_{ABF}, N_{ABF}): lower the value, better is the quality.

VI. Experimental Results and Discussions

Results of fusion using the three proposed methods are compared with twelve existing techniques. First two methods are spatial domain fusion using $Mean$ and $Maximum$ fusion rule respectively, where fused pixel is average/maximum of source pixels. Wavelet (DWT) [2] and Curvelet-Wavelet ($CVT - DWT$) [1] are two of the best recent methods of multifocus image fusion. DWT [5] and Wavelet Packet ($DWPT$) [6] are methods used for medical image fusion, whereas $DWPT$ [8] and Contourlet (CNT) [7] are methods for fusing multispectral surveillance images. Besides these, we have also compared the results with fusion using DWT, $DWPT$, curvelet (CVT) and CNT with $'mean - max'$ fusion rule where for low frequency coefficients average, and for high frequency coefficient maximum of the source coefficients is taken as the fused coefficient [8].

We have experimented with several standard test pairs of multifocus images provided by ImageFusion.org. However, as the results were consistent with all the test images, results of only one of the pairs namely $'clock'$ shown in Figure 1, are discussed and tabulated (Table I) in this paper. We have also generated our own database of simulated multifocus image pairs by processing well focused images, so that for these pairs ground truth can be made available and performance evaluation can be complete in true sense. One of such pair generated from well-known $'Lena'$ image (size 512×512), is shown in Figure 5 (a)-(b). For generating these simulated multifocus images, we first took a well focused image which can be used as the 'ground truth' (GT) and created two masks, one for the foreground and one for the background. Then to generate first simulated multifocus source image, we blurred the background using Gaussian blur keeping foreground in focus and for second source image we kept original background in focus and blurred the foreground. The respective evaluating parameters are reported in Table II and image results are given in Figure 5.

Existing contourlet based multifusion fusion technique (CNT [7]), has one of the highest value for *Gradient* indicating the sharpest fused image, but both the methods also have the lowest $Petrovic$ quality (Q_{ABF}) value. This clearly shows that the $Gradient$ can not be a good measure of performance always, as its value can be higher due to artifacts also, which can be disastrous. The other existing multifocus fusion [1] gives relatively higher quality (Q_{ABF}) but at the cost of producing higher noise (N_{ABF}. All other existing techniques give poor quality and / or high noise, and hence not suitable for multifocus image fusion. However, the proposed methods give the highest value for Q_{ABF} indicating that edge information is preserved very well. The major achievement is the significantly lowest noise (N_{ABF}) value, which the most desired quality of an efficient fusion technique. The proposed techniques also have high values for $Entropy$, $Mutual\ Information$, $Fusion\ Symmetry$ and $Correlation$, indicating increase in relevant information. Visual quality of proposed fusion is also clearly superior as seen in Figure 4 and 5.

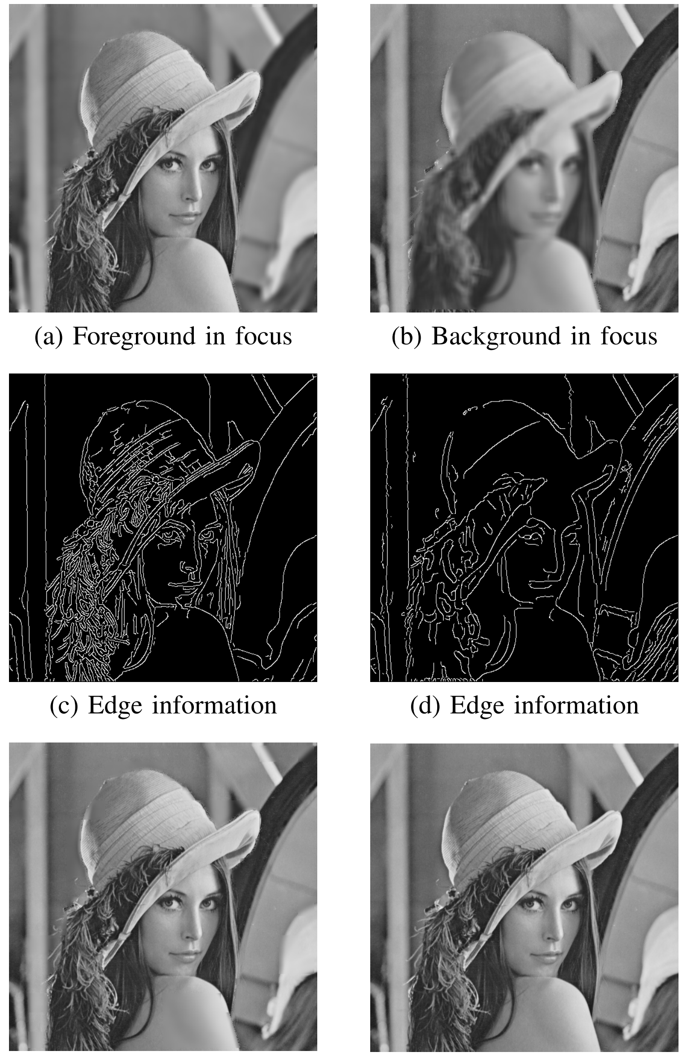

(a) Foreground in focus (b) Background in focus

(c) Edge information (d) Edge information

(e) Fused image (f) Ground truth

Fig. 5. Simulated multifocus source images of *'Lena'* [10]: (a) foreground in focus (b) background in focus; respective edge informations are depicted in (c) and (d); (e) final fused image using the proposed $ABS-AT$ fusion

VII. Conclusions

The experimental results show that the fusion technique developed for other class of images (e.g. medical, multispectral) may not do equally good for multifocus image fusion. It also show that the proposed fusion techniuqe is well suited for fusion of multifocus images in spatial domain. The method shows significant improvement over existing multifocus image fusion methods, outperforming in all the evaluation indices, as can be seen from the results given in Table I with best values for all the $Petrovic$ metrics. The major achievements of the proposed method is minimum artifacts (lowest N_{ABF}) and maximum edge preservation (highest Q_{ABF}). This is a significant achievement, as artifacts may lead to wrong interpretations which can be catastrophic, especially in applications like surveillance where it can result into false alarms. In addition, the proposed method also yield excellent sharpness, clarity and edge preservation along with increase in mutual information, fusion symmetry and correlation; hence giving better visual quality.

VIII. Acknowledgements

This work was supported by Microsoft Research India under the MSRI PhD Fellowship Award 2008.

References

[1] Shutao Li, Bin Yang, "Multifocus Image Fusion by Combining Curvelet and Wavelet Transform," *Pattern Recognition Letters*, vol.29, pp.1295–1301, 2008.

[2] S. Arivazhagan, L. Ganesan, T. G. Subash Kumar, "A modified statistical approach for image fusion using wavelet transform," *Springer Journal SIViP*, Vol.3, pp. 137–144, 2009.

[3] A. Goshtasby, "Fusion of multi-exposure images," *Image and Vision Computing*, vol. 23, no. 6, pp. 611–618, 2005.

[4] X. Yang, W. Yang, J. Pei, "Different focus points images fusion based on wavelet decomposition," in Proc. of *International Conference on Information Fusion*, vol.1, pp. 3–8, 2000.

[5] CHENG Shangli, H. Junmin, L. Zhongwei, "Medical Image of PET/CT Weighted Fusion Based on Wavelet Transform," in Proc. of *International Conference on Bioinformatics and Biomedical Engineering (ICBBE)*, pp. 2523–2525, 2008.

[6] Yang Licai, L. Xin, Y Yucui, Medical Image Fusion Based on Wavelet Packet Transform and Self-adaptive Operator, in Proc. of *International Conference on Bioinformatics and Biomedical Engineering (ICBBE)*, pp. 2647–2650, 2008.

[7] Soad Ibrahim, Michael Wirth, "Visible and IR Data Fusion Technique Using the Contourlet Transform," in Proc. of *IEEE International Conference on Computational Science and Engineering*, pp. 42–47, 2009.

[8] Parul Shah, S. N. Merchant, U. B. Desai, "Fusion of Surveillance Images in Infrared and Visible Band using Curvelet, Wavelet and Wavelet Packet Transform," *International Journal of Wavelets, Multiresolution and Information Processing (IJWMIP)*, vol. 8, no. 2, pp. 271–292, 2010.

[9] J.F Canny, "A computational approach to edge detection," *IEEE Trans Pattern Analysis and Machine Intelligence*, vol.8, no. 6, pp 679–698, Nov 1986.

[10] http://www.imagefusion.org

[11] Yang Licai, L. Xin, Y Yucui, "Medical image fusion based on wavelet packet transform and self-adaptive operator," in Proc. *2nd International*

TABLE I
PERFORMANCE COMPARISON OF FUSION RESULTS FOR SIMULATED MULTIFOCUS $'clock'$ IMAGE PAIRS

	μ	σ	$\overline{G}$	H	MI	FS	$CORR$	Q_{ABF}	L_{ABF}	N_{ABF}
$Mean$	97.273	49.346	3.69	7.26	5.296	1.84	0.989	0.589	0.401	0.001
$Maximum$	101.037	50.197	3.63	7.27	7.467	1.84	0.98	0.526	0.247	0.327
$DWT(mean-max)$ [8]	97.109	50.482	6.057	7.313	4.176	1.674	0.982	0.609	0.247	0.327
DWT [2]	96.857	50.327	5.619	7.303	4.363	1.634	0.982	0.57	0.292	0.338
DWT [5]	97.181	49.593	4.714	7.284	4.039	1.504	0.985	0.582	0.333	0.309
$DWPT(mean-max)$ [8]	97.076	49.513	5.108	7.282	4.977	1.838	0.985	0.462	0.424	0.141
$DWPT$ [6]	97.827	50.114	5.685	7.305	3.962	1.632	0.979	0.582	0.271	0.368
$DWPT$ [8]	96.828	50.125	4.875	7.277	4.508	1.728	0.984	0.604	0.348	0.063
$CVT(mean-max)$ [8]	98.565	49.119	4.566	7.414	4.007	1.838	0.985	0.463	0.436	0.092
$CVT-DWT$ [1]	99.147	52.078	5.807	7.425	4.319	1.733	0.98	0.658	0.227	0.387
$CNT(mean-max)$	97.097	50.117	8.538	7.468	3.885	1.871	0.972	0.302	0.406	0.158
CNT [7]	98.923	49.906	8.56	7.478	3.726	1.843	0.97	0.314	0.409	0.158
Proposed Fusion Techniques										
$FBS-AT$	96.646	50.667	5.126	7.263	7.3	1.872	0.978	0.69	0.161	0.0003
$ABS-AT$	96.671	50.739	5.34	7.278	5.425	1.582	0.978	0.705	0.141	0.001

TABLE II
PERFORMANCE COMPARISON OF FUSION RESULTS FOR SIMULATED MULTIFOCUS $'Lena'$ IMAGE PAIRS

	μ	σ	$\overline{G}$	H	MI	FS	$CORR$	Q_{ABF}	L_{ABF}	N_{ABF}
$Ground\ Truth$	124.109	47.941	8.932	7.447	6.175	1.844	0.979	0.77	–	–
$Mean$	124.111	45.412	5.258	7.356	5.24	1.88	0.989	0.575	0.422	0.0003
$Maximum$	128.146	44.864	5.916	7.373	8.677	1.972	0.981	0.579	0.383	0.0115
$DWT_{(mean-max)}$ [8]	124.115	47.012	9.25	7.438	5.209	1.924	0.979	0.66	0.256	0.18
DWT [2]	124.204	47.484	9.059	7.436	5.887	1.915	0.979	0.68	0.193	0.053
DWT [5]	124.084	45.215	5.23	7.377	4.132	1.492	0.982	0.426	0.522	0.205
$DWPT_{(mean-max)}$ [8]	124.124	45.716	7.45	7.382	4.37	1.809	0.982	0.476	0.48	0.06
$DWPT$ [6]	124.742	46.917	9.115	7.433	5.345	1.929	0.978	0.654	0.216	0.056
$DWPT$ [8]	124.155	46.027	8.117	7.383	5.234	1.909	0.985	0.646	0.317	0.025
$CVT_{(mean-max)}$ [8]	124.687	45.593	5.988	7.384	4.665	1.867	0.986	0.496	0.448	0.049
$CVT-DWT$ [1]	124.352	47.949	9.059	7.449	4.189	1.594	0.979	0.706	0.209	0.399
$CNT_{(mean-max)}$	124.094	46.407	10.632	7.49	3.773	1.888	0.967	0.365	0.422	0.043
CNT [7]	125.157	46.479	10.661	7.497	3.693	1.878	0.967	0.309	0.423	0.046
Proposed Fusion Technique										
$ABS-AT$	124.163	47.528	8.726	7.434	7.199	1.963	0.978	0.765	0.114	0.006

Conference on Bioinformatics and Biomedical Engineering (ICBBE), pp. 2647–2650, 2008.

[12] Z. Zhong, R.S. Blum, "A categorization of multiscale decomposition-based image fusion schemes with a performance study for a digital camera application, *IEEE Proceeding*, vol.87, pp. 1315–1326, 1999.

[13] Seetha M., MuraliKrishna I.V., Deekshatulu B.L., Data fusion performance analysis based on conventional and wavelet transform techniques, in Proc. *IEEE International Geoscience and Remote Sensing Symposium*, vol. 4, pp. 2842–2845, 2005.

[14] G. Qu, Dali Zhang, Pingfan Yan, "Information measure for performance of image fusion," *Electronics Letters*, vol.38, pp. 313–315, 2002.

[15] V Petrovic and C Xydeas, "Objective Image Fusion Performance Characterisation," *ICCV'05*, pp. 1866–1871, 2005.